

# MANSOURA JOURNAL OF CHEMISTRY

Official Journal of Faculty of Science, Mansoura University, Egypt

E-mail: scimag@mans.edu.eg ISSN: 2974-4938



# Fabrication of a new cobalt(II) complex by a nitrogenous substituted pyridinone ligand and its antitumor profile

Dina S. Sheliel<sup>a,\*</sup>, Eslam A. Ghaith<sup>a,b</sup>, Usama El-Ayaan<sup>a</sup>, Nagwa Nawar<sup>a</sup>

<sup>a</sup> Chemistry Department, Faculty of Science, Mansoura University, ET-35516-Mansoura, Egypt.

\* Correspondence: Email: Dinaelsayed@mans.edu.eg

Received:9/10/2025 Accepted:22/10/2025

**Abstract:** A new chelate of a nitrogenous substituted pyridinone ligand, designated as [Co(AHPO)(H<sub>2</sub>O)<sub>2</sub>(OAc)<sub>2</sub>].3H<sub>2</sub>O, has been prepared. The structural properties of this novel compound were completely characterized via a variety of methods, such as FT-IR, CHN analyses, and UV-visible spectroscopy. FTIR revealed that The AHPO ligand works as a neutral, OO, bidentate ligand chelating the Co(II) ion through both the oxygen atoms of the carbonyl groups. Furthermore, magnetic and molar conductance conductometric were measured. The analysis of the isolated [Co(AHPO)(H<sub>2</sub>O)<sub>2</sub>(OAc)<sub>2</sub>].3H<sub>2</sub>O chelate exhibited negligible molar conductance affirming the non-electrolytic behavior of Co(II) complex and the existence of acetate anion inside the coordination sphere. Also, thermal TG and DTG methods were employed. Whereas Coats-Redfern and Horowitz-Metzger models were applied to evaluate the thermodynamic and kinetic parameters of the Co(II) complex. Eventually, the in vitro antitumor screening of the investigated [Co(AHPO)(H<sub>2</sub>O)<sub>2</sub>(OAc)<sub>2</sub>].3H<sub>2</sub>O complex was examined against two different cell lines. This encompassed liver cancer (HePG-2) and breast cancer (MCF-7).

keywords: Pyridinone, Co(II) complex, Antitumor properties, Kinetic studies.

## 1. Introduction

Nitrogen and oxygen-containing compounds show crucial roles in various biochemical and pharmacological processes, exhibiting diverse biological activities. These compounds are known to exhibit potent biomedical effects, and their incorporation in metal complexes can modulate reactivity, stability, and biological interactions. The existence of nitrogen and oxygen donor atoms facilitates the formation of metal complexes with tailored properties, making them promising candidates for therapeutic applications, including antioxidant, antimicrobial, and anticancer activities [1-3].

On the other hand, DHA (dehydroacetic acid) is extensively utilized as a preservative, fungicide, and pesticide [4]. This results from several intriguing characteristics, including minimal volatility, excellent stability, and potent antibacterial activity against molds, yeasts, and bacteria [5]. Whereby, DHA serves as a stabilizer for Vitamin C, notably beneficial in the food sector, and functions as an anti-

enzyme agent, utilized in toothpastes to mitigate pickle bloating [6-8].

Furthermore. DHA derivatives biologically active molecules in organic synthesis, principally as preliminary substances for the fabrication of numerous Mannich bases, Schiff bases, chalcones, etc. Whereas the DHA Schiff bases and their metal chelates possess a diversity of uses in the analytical, biological, and pharmaceutical fields [9]. Countless researchers recorded the biological properties of different metal compounds prepared from DHA Schiff bases, viz., synergistic, anti-viral, anti-inflammatory, analgesic, anti-oxidant, antidiabetic, antitumor, anti-fertility, cytotoxic, and DNA photocleavage properties [10].

In this study, we designed and prepared a new Co(II) complex from DHA derivative, and its antitumor potencies were discovered.

<sup>&</sup>lt;sup>b</sup> Department of Chemistry, Faculty of Science, New Mansoura University, New Mansoura City, Egypt.

## 2. Experimental

## 2.1. materials and reagents

DHA, *o*-phenylene diamine, DMSO, absolute ethanol and Co(OAC)<sub>2</sub>.4H<sub>2</sub>O were obtained from different suppliers, including BDH, Sigma-Aldrich, and Merck.

# 2.2 Characterization techniques

CHN analyses were conducted by a Perkin-Elmer 2400 series II analyzer. The amount of evaluated through copper(II) was volumetric technique [11]. FTIR spectroscopy performed using a Bruker FT-IR spectrometer (Invenio S, Germany) in the (4000-400 cm<sup>-1</sup>) region. At ambient temperature, the Sherwood magnetic susceptibility balance was applied to determine the magnetic susceptibility of the Co(II) complex. Furthermore, the electronic spectrum attained UV2 Unicam on a spectrophotometer utilizing DMSO as TG-50 solvent. Whereas, Shimadzu thermogravimetric analyzer from 20 °C to 800 °C with heating rate (10 °C/min) and dynamic atmosphere (20 mL/min) conducted to evaluate TG/DTG analyses.

Additionally, AJENCO, Vision Plus EC 3175 conductivity meter was used to measure the molar conductance of the Co(II) complex.

### 2.3. Synthesis of Co(II) complex

1 mmol of solid (AHPO) ligand was refluxed with 1 mmol of Co(OAC)<sub>2</sub>.4H<sub>2</sub>O salt for 5 hours in an ethanolic solution. The precipitate was then separated, filtered, washed, and well dried. Table 1 contains the most important data of the Co(II) complex.

**Table 1**: The Analytical and physical data of [Co(AHPO)(H<sub>2</sub>O)<sub>2</sub>(OAc)<sub>2</sub>].3H<sub>2</sub>O complex.

Complex (Empirical formula)	Mwt. (g mol <sup>-1</sup> )	Color	% Found (% Calculated)				
			C	H	N	M	
$C_{18}H_{30}C \\ oN_2O_{12}$	525.37	Reddish brown	41.21 (41.15)	5.64 (5.76)	5.47 (5.33)	11.10 (11.22)	

## 2.4. Antitumor properties

The *in vitro* antitumor examination of the new Co(II) complex was performed against HepG-2 (Hepatocellular cancer) as well as MCF-7 (breast cancer) using the MTT colorimetric assay at 570 nm, following the reported method [12].

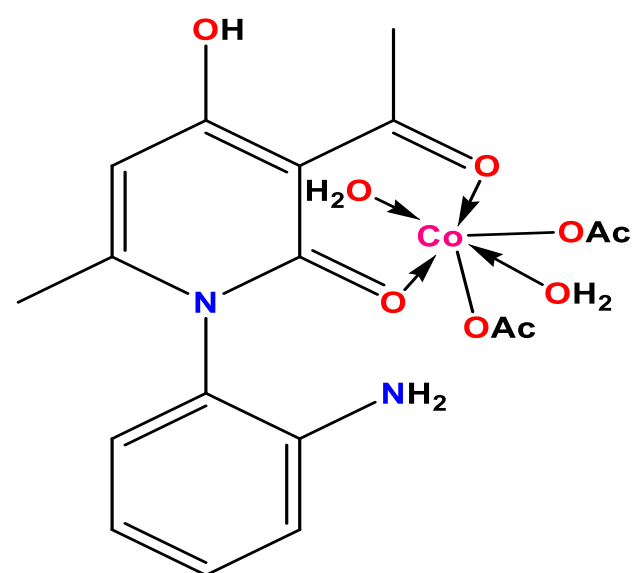


**Figure 1**: The proposed structure of  $[Co(AHPO)(H_2O)_2(OAc)_2].3H_2O$  complex.

## 3. Results and discussion

#### 3.1. Molar conductance measurements

The conductometric analysis of the isolated  $[Co(AHPO)(H_2O)_2(OAc)_2].3H_2O$  chelate was executed in (0.001 M) DMSO solution. The results exhibited negligible molar conductance  $(\Lambda m = 3.577 \text{ Ohm}^{-1}\text{cm}^2\text{mol}^{-1})$ , which was detected, affirming the non-electrolytic behavior of Co(II) complex and the existence of acetate anion inside the coordination sphere [13].

# 3.2. FT-IR spectroscopy

infrared spectrum of  $[Co(AHPO)(H_2O)_2(OAc)_2].3H_2O$ chelate clarified in Figure 2. Neutral OO bidentate criteria of the AHPO ligand happen for the Co(II) complex. This is affirmed by the shift of the ketonic carbonyl group from 1698 cm<sup>-1</sup> to 1664 cm<sup>-1</sup> and the lactamic group from 1634 cm<sup>-1</sup> to 1644 cm<sup>-1</sup>. Whereas, a new band is noticed at 517 cm<sup>-1</sup>, which can be ascribed to v(Co-O). The spectrum revealed a broad absorption peak at 3450 cm<sup>-1</sup> attributed to υ(OH) of solvation or coordination water molecules and confirmed via TG thermal techniques. Whereby, both the symmetric and

asymmetric peaks of the monodentate acetate group are recognized at 1590 cm<sup>-1</sup> and 1345 cm<sup>-1</sup> (with a difference of 245 cm<sup>-1</sup>), individually. The AHPO ligand works as a neutral OO bidentate ligand chelating the Co(II) ion through both the oxygen atoms of the carbonyl groups [14].

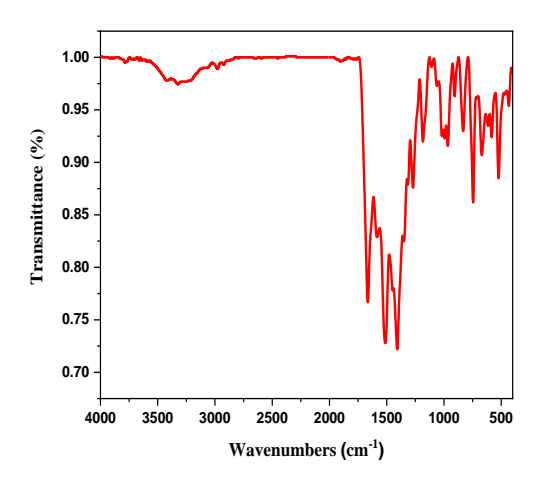


**Figure 2**: IR spectrum of [Co(AHPO)(H<sub>2</sub>O)<sub>2</sub>(OAc)<sub>2</sub>].3H<sub>2</sub>O complex.

## 3.3. UV-visible and magnetic moment studies

Hexa-coordination configuration for  $[Co(AHPO)(H_2O)_2(OAc)_2].3H_2O$  chelate supposed, based on the presence of 446 nm and 510 nm which are ascribed to  ${}^{4}T_{1}g$  (F)  $\rightarrow$  ${}^{4}T_{1}g(P)$  (v<sub>3</sub>) and  ${}^{4}T_{1}g$  (F)  $\rightarrow {}^{4}A_{2}g(F)$  (v<sub>2</sub>), separately, in high-spin octahedral a environment around the Co(II) ion. While the three peaks in the region 242-396 nm are concerned with LMCT. Whereby, the value of the magnetic moment (4.96 B.M.) is proof of the high-spin octahedral environment around the Co(II) ion. [15].

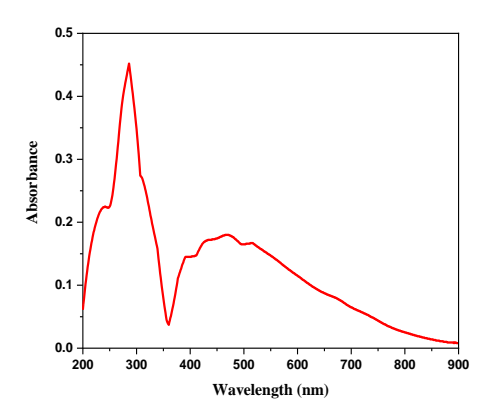


**Figure 3**: Electronic absorption spectrum of [Co(AHPO)(H<sub>2</sub>O)<sub>2</sub>(OAc)<sub>2</sub>].3H<sub>2</sub>O complex.

## 3.4. Thermal studies

of curve  $[Co(AHPO)(H_2O)_2(OAc)_2].3H_2O$ exemplified in Figure 4, discloses four discrete steps of thermal degradation. This is extra explained in Table 2. The first phase (Found:10.063%; Calculated: 10.287 %) within the temperature range of 30 to 120 °C shows a loss equivalent to 3H<sub>2</sub>O. Then, the next step (Found: 56.737 %; Calculated: 56.390 %) happened within the temperature range of 120 to 498 °C, matching with the loss of two mole of coordinated water and a C<sub>13</sub>H<sub>10</sub>NO<sub>5</sub> moiety. Whereby, the third stage (Found: 15.052 %; Calculated:14.488 %) noticed between 498 and 627 °C was allied to the loss of C<sub>3</sub>H<sub>10</sub>NO fragment. Finally, the residual part (Found: 18.148 %; Calculated.: 18.836%) refers to C<sub>2</sub>CoO fragment.

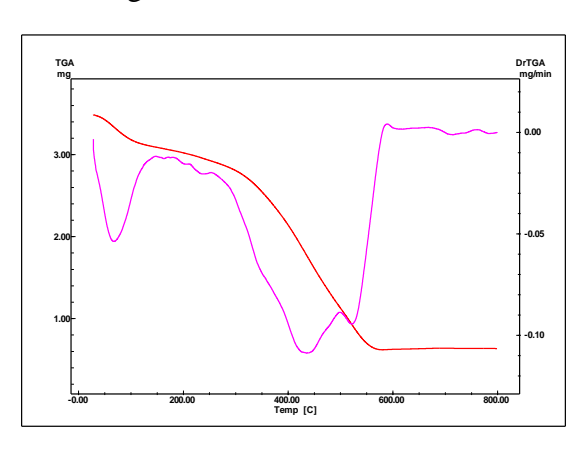


**Figure 4:** TG / DTG plots of  $[Co(AHPO)(H_2O)_2(OAc)_2].3H_2O$  complex.

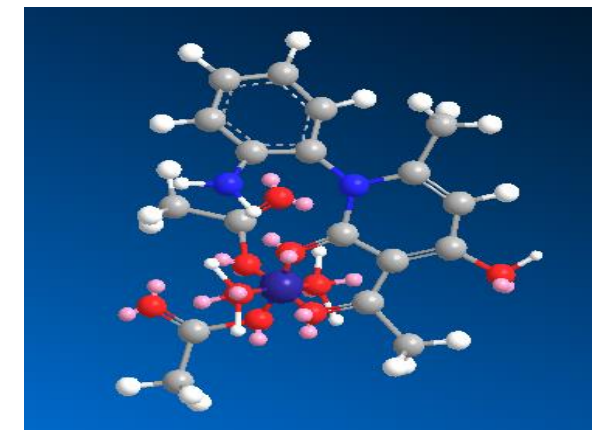
**Table 2**: Degradation steps for  $[Co(AHPO)(H_2O)_2(OAc)_2].3H_2O$  complex within the temperature range (°C) and weight loss.

75			Wt. Loss		
Compoun	Temp. range (°C)	Removed	%Found	%Calcul ated	
	30-120	(3H <sub>2</sub> O)	10.063	10.287	
[Co(AHPC )(H <sub>2</sub> O) <sub>2</sub> (O Ac) <sub>2</sub> ].3H <sub>2</sub> (	120-498	$(2H_2O + C_{13}H_{10}NO_5)$	56.737	56.390	
[Co(A) )(H <sub>2</sub> C	498-627	$(C_3H_{10}NO)$	15.052	14.487	
) × ¥	627-800	(CoO + 2C)	18.148	18.836	

#### 3.5. Kinetic studies

The thermodynamic and kinetic parameters were calculated *via* the Eyring equations [16, 17]. The data introduced in **Table 3** proposes

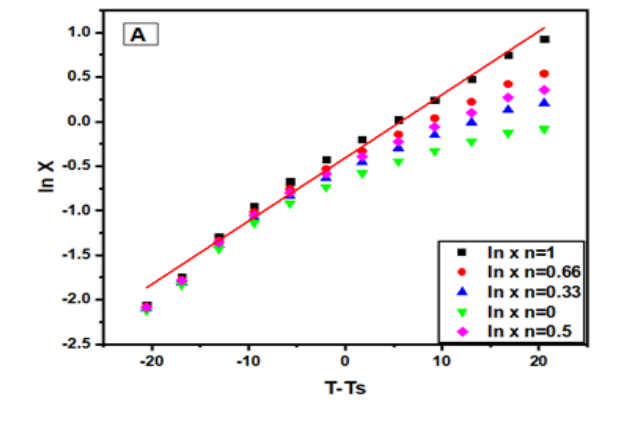
that the degradation phases are endothermic, as specified by the positive  $\Delta H^*$ Additionally, most of the degradation steps exhibit negative signs for the entropy ( $\Delta S^*$ ), which infers that the reactants are less ordered than the activated complex. Finally, the positive signs of Gibbs free energy ( $\Delta G^*$ ) affirm the non-spontaneous decomposition steps. Whereby, Figure 6 exemplifies the Coats-Redfern and Horowitz-Metzger graphs for the  $[Co(AHPO)(H_2O)_2(OAc)_2].3H_2O$ describing the (a) first, (b) second, and (c) third degradation steps.

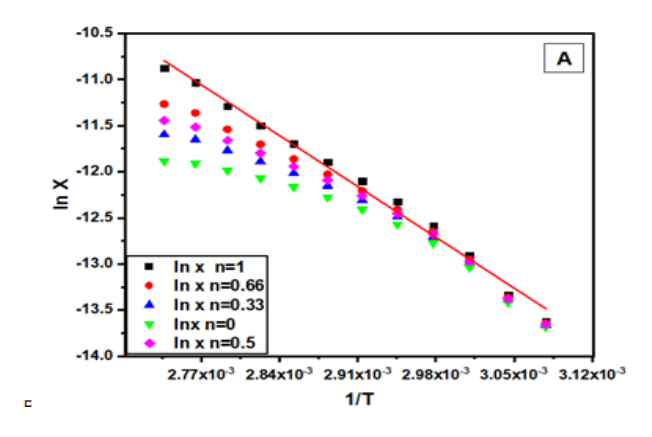


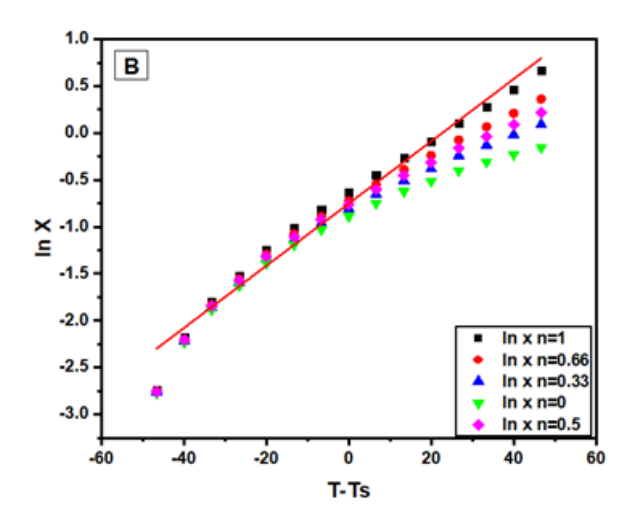
**Figure 5:** 3D structure of [Co(AHPO)(H<sub>2</sub>O)<sub>2</sub>(OAc)<sub>2</sub>].3H<sub>2</sub>O complex.

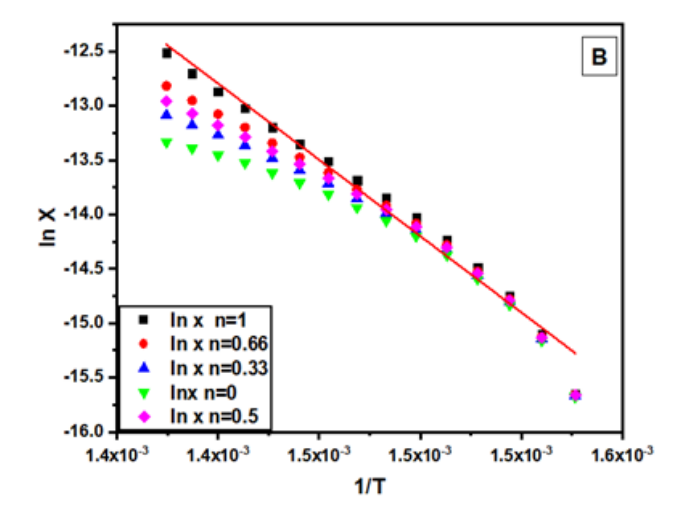
**Table 3**: Kinetic Parameters assessed *via* Horowitz-Metzger and Coats-Redfern models for  $[Co(AHPO)(H_2O)_2(OAc)_2].3H_2O$  complex.

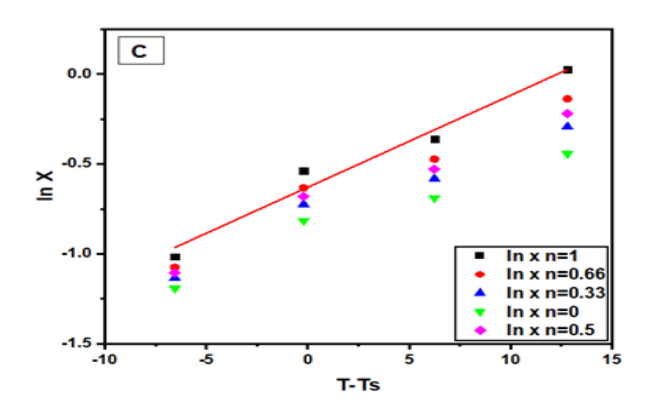
Method	Peak	Mid Temp. (K)	E <sub>a</sub> KJ/mol	A (S <sup>-1</sup> )	ΔH <sup>*</sup> KJ/mol	ΔS* KJ/mol.K	ΔG <sup>*</sup> KJ/mol
Coats-Redfern method	1 <sup>st</sup>	343	64.33	67214575	61.72	-96.22	94.70
	2 <sup>nd</sup>	660	116.71	3339443	111.23	-126.63	194.79
	3 <sup>rd</sup>	800	505.01	9.5E+30	498.36	339.91	226.41
Horowitz-Metzger method	1 <sup>st</sup>	343	69.33	4.4E+08	66.48	-80.60	94.09
	2 <sup>nd</sup>	660	120.14	12664015	114.65	-115.55	190.91
	3 <sup>rd</sup>	800	272.43	4.18E+15	265.78	45.92	229.04











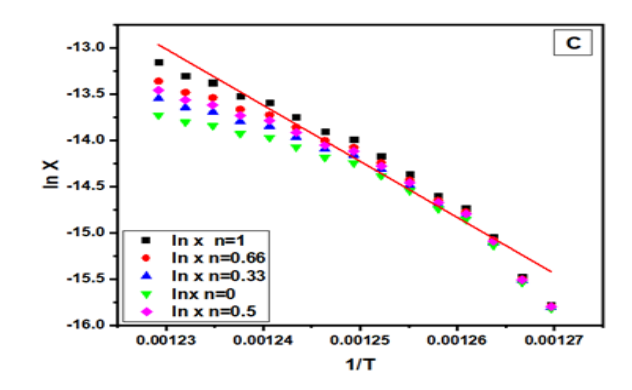


**Figure 6**: The Horowitz-Metzger and Coats-Redfern graphs for the [Co(AHPO)(H<sub>2</sub>O)<sub>2</sub>(OAc)<sub>2</sub>].3H<sub>2</sub>O complex, describing the (a) first, (b) second, and (c) third degradation steps.

## 3.6. Biological efficacy

#### 3.6.1. Antitumor studies

The in vitro antitumor screening of the investigated [Co(AHPO)(H<sub>2</sub>O)<sub>2</sub>(OAc)<sub>2</sub>].3H<sub>2</sub>O complex was examined against two different cell lines. This encompassed liver cancer (HePG-2) and breast cancer (MCF-7). Additionally, Doxorubicin (a positive control) exposed a powerful anticancer property with  $IC_{50}$  (µM) equal to  $4.50\pm0.2$  and  $4.17\pm0.2$  in the case of HepG-2 and MCF-7, respectively. Whereby, the studied complex revealed weak anticancer activity with IC<sub>50</sub> (µM): 75.42±3.7 in case of MCF-7and 87.10±4.4 in case of HePG-2. The weak antitumor performance of Co(II) compound may be due to the insufficient accumulation in cancer cells, degradation, rapid metabolism, lack of effective interaction with cellular targets, poor cell membrane penetration, or the presence of resistance mechanisms in the cancer cells [18,19].

#### **Conclusion**

In the present work, we successfully separated a new Co(II) chelate that is generated from the 3-acetyl-1-(2-aminophenyl)-4-hydroxy-6-methylpyridin-2(1H)-one (AHPO) ligand. The outcomes verified that the newly studied chelate showed an octahedral stereochemistry surrounding the Co(II) ion.

Additionally, the data of the infrared analysis proposed that the AHPO ligand operated as a neutral bidentate (OO) ligand in coordination with the Co(II) center. Whereas the thermal characterizations explicated the quantification of crystalline and coordination

water molecules. Furthermore, the thermodynamic and kinetic parameters were established by the Eyring equations. Eventually, the antitumor effectiveness of the examined compound was critically screened for both MCF-7 and HePG-2 cell lines.

#### References

- 1. E.A. Ghaith, M A. El Salam, G. E. Said (2025) Barbiturate and uracils scaffolds as potential insectidal agents: Synthesis, DFT Studies and in vivo Biochemical susceptibility of the polyphagous pest, cotton leafworm, Spodopetra littoralis (Lidopetra Noctuidae, *Journal of Molecular Structure* 1348 142302.
- 2. D.S. Sheliel, E.A. Ghaith, U. El-Ayaan, N. Nawar, (2025) Structure Elucidation, Cyclic Voltammetry, Fluorescence, DFT, Biological Potency, and In Silico Profiling of New Bivalent Transition Metal Coordination Compounds of 7-amino-4*H*-pyrazolo [3, 4-b] pyridinone Ligand, *Journal of Molecular Structure* 1348 143427.
- 3. E.A. Ghaith, A.B. Abdallah, A.A.El-Sawi, G.G.El-bana, (2025) Ultrasound-assisted utility of 1,2,4-triazole as a multisite-sequential scaffold to construct different heterocycles, Accredited by molecular modeling and electrochemical studies, *Journal of Heterocyclic Chemistry*, **62**, 505-512.
- 4. A. Grover, A. Kumar, R.K. Tittal, K. Lal, (2024) Dehydroacetic acid a privileged medicinal scaffold: A concise review, Archiv der Pharmazie **357(2)** 2300512.

- S. De Vaugelade, E. Nicol, S. Vujovic, S. 5. Bourcier, S. Pirnay, S. Bouchonnet, (2018)Ultraviolet-visible phototransformation of dehydroacetic acid-Structural characterization of photoproducts and global ecotoxicity, Rapid Communications Mass Spectrometry 32(11) 862-870.
- 6. M.V. Cooke, G.M. Chans, G. A. Argüello, W.J. Peláez, (2020) Photolysis, tautomerism and conformational analysis of dehydroacetic acid and a comparison with 2-hydroxyacetophenone and 2-acetyl-1, 3 cyclohexanodione, Heliyon 6(7).
- 7. J.N. Asegbeloyin, P.M. Ejikeme, L.O. Olasunkanmi, A.S. Adekunle, E.E. Ebenso, A Novel Schiff Base of 3-acetyl-4-hydroxy-6-methyl-(2H) pyran-2-one and 2, 2'-(ethylenedioxy) diethylamine as Potential Corrosion Inhibitor for Mild Steel in Acidic Medium, Materials 8(6) (2015)2918-2934.
- 8. A. PS, D.A. Thadathil, L. George, A. Varghese, (2024) Food Additives and Evolved Methods of Detection: A Review, Critical Reviews in Analytical Chemistry 1-20.
- 9. W.S. Hamama, E.A. Ghaith, M.E. Ibrahim, M. Sawamura, H.H. Zoorob, (2021), Synthesis of 4-Hydroxy-2-pyridinone Derivatives and Evaluation of Their Antioxidant/Anticancer Activities, Chemistry Select, **6(7)** (2021) 1430-1439.
- 10. E.A. Ghaith, H.H. Zoorob, M.E. Ibrahim, M. Sawamura, W.S. Hamama, (2020) Convenient synthesis of binary and fused pyrazole ring systems: accredited by molecular modeling and biological evaluation, ChemistrySelect **5(47)**, 14917-14923.
- 11. G.H. Jeffery, (2022) Vogel's Textbook of Quantitative Chemical Analysis 5th Ed (A John Wiley & Sons, INC).
- 12. F. Denizot, R. Lang, (1986) Rapid colorimetric assay for cell growth and survival: modifications to the tetrazolium dye procedure giving improved sensitivity and reliability, *Journal of immunological methods* **89(2)** 271-277.
- 13. W.J. Geary, (1971) The use of conductivity measurements in organic

- solvents for the characterization of coordination compounds, Coordination Chemistry Reviews **7(1)** 81-122.
- 14. K. Nakamoto, (2009) Infrared and Raman spectra of inorganic and coordination compounds, part B: applications in coordination, organometallic, and bioinorganic chemistry, John Wiley & Sons.
- 15. A.B.P. Lever, (1968) Inorganic electronic spectroscopy, Elsevier, Amsterdam.
- 16. A. Coats, J. Redfern, (1964) Kinetic parameters from thermogravimetric data, Nature **201** (**4914**) 68-69.
- 17. H.H. Horowitz, G. Metzeger, (1963) A new analysis of thermogravimetric traces, Analytical Chemistry **35** (**10**) 1464-1468.
- 18. T. Haider, V. Pandey, N. Banjare, P.N. Gupta, V. Soni, (2020) Drug resistance in cancer: mechanisms and tackling strategies, Pharmacological Reports **72**(5) 1125-1151.
- 19. D.S. Sheliel, U. El-Ayaan, N. Nawar, (2021) Synthesis of new Ni(II) complex of curcumin arginine ligand and evaluation of its antimicrobial potency, Mansoura *Journal of Chemistry* **53(3)** 33-38.